

Strongly correlated quantum dots in weak confinement potentials and magnetic fields

Min-Chul Cha^a and S.-R. Eric Yang^b

^a Department of Physics, Hanyang University, Ansan 425-791, Korea

^b Department of Physics, Korea University, Seoul, Korea

(Dated: October 22, 2018)

We explore a strongly correlated quantum dot in the presence of a weak confinement potential and a weak magnetic field. Our exact diagonalization studies show that the ground state property of such a quantum dot is rather sensitive to the magnetic field and the strength of the confinement potential. We have determined rich phase diagrams of these quantum dots. Some experimental consequences of the obtained phase diagrams are discussed.

PACS numbers: 73.21.La, 73.23.Hk

Fabrication of quantum dots has reached such an advanced state that the shape of the confinement potential and the number of electrons in them can be tuned precisely [1]. Ground states of isolated quantum dots fabricated from 2D electron systems can display various strong correlation effects. Quantum Hall related ground states have been explored in the strong magnetic field limit [2, 3], and Hund's rule for shell structures for a two-dimensional harmonic potential has been investigated [4]. Recently transport through a quantum dot has attracted much attention, especially Kondo related physics [5]. Wigner crystal states and strong electron correlation in quantum dots have been explored through various methods[6, 7]

In this paper we explore possible ground states of an isolated quantum dot made of dilute 2D electron systems in the presence of a weak magnetic field. Recently unusual behavior suggestive of a metal-insulator transition has been reported in a variety of dilute two-dimensional electron and hole systems [8], where the dimensionless parameter $R = E_{e-e}/E_s \gg 1$ (here E_{e-e} is the electron-electron interaction energy and E_s is the characteristic single particle energy). Strong electron correlation effects are expected to be play an important role in these systems. Quantum dots fabricated from dilute 2D electron systems are also expected to exhibit strong electron correlation effects. Here we focus on how the ground state spin depends on the applied magnetic field and the strength of the confinement potential. To describe properly the delicate competition[9] between different spins states in strongly correlated regime non-perturbative methods[2, 10, 11, 12] are required. We adopt exact diagonalization methods[2, 10, 11] since various mean field theoretical methods[13] are applicable only in the regime $R < 1$.

We model a quantum dot as follows. Electrons move on a 2D plane under the influence of a parabolic confinement potential and a weak magnetic field applied perpendicular to the plane. In parabolic quantum dots, the ratio R can be characterized by $(e^2/\kappa a)/\hbar\Omega$ where a is the typical lateral size of the dot, κ the dielectric constant, and Ω the confining frequency of the harmonic potential. We consider up to six electrons in the parameter regime $R \sim 5 - 16$. We find that the ground state of quantum

dots for these values of R is rather sensitive to the magnetic field and the strength of the confinement potential. Our investigation suggests that this is a direct consequence of strong electron correlation: it originates from the existence of nearly degenerate quantum dot eigenstates. We obtain rich phase diagrams of these quantum dots and discuss experimental consequences.

Electrons of the dot is confined by a harmonic potential $V(r) = \frac{1}{2}m^*\Omega^2r^2$, where m^* is the effective electron mass. A magnetic field B is applied along the z -axis through a vector potential in a symmetric gauge. We include also the Zeeman splitting, $g\mu B[\text{meV}] = 0.026B[\text{T}]$. We take the Hamiltonian of N electron dot to be $H = \sum_{i=1}^N H_i + H_{int}$, where the single particle Hamiltonian is modeled by

$$H_i = \frac{\mathbf{p}_i^2}{2m^*} + \frac{1}{2}m^*\omega^2r_i^2 - \frac{1}{2}\omega_c\mathbf{l}_i \cdot \hat{\mathbf{B}} - g\mu BS_{z,i}, \quad (1)$$

and where the many-body interaction term is given by

$$H_{int} = \frac{1}{2} \sum_{i \neq j}^N \frac{e^2}{\kappa|\mathbf{r}_i - \mathbf{r}_j|}. \quad (2)$$

Here $\kappa = 12.4$ and ω_c are the dielectric constant of GaAs semiconductor and cyclotron frequency. The eigenfunctions[14, 15] of the single particle Hamiltonian are

$$\phi_{nl_{s_z}}(\mathbf{r}) = \frac{1}{\sqrt{2\pi a}} e^{-il\theta} R_{nl}\left(\frac{r^2}{2a^2}\right) \chi_{s_z} \quad (3)$$

where $a^2 = \hbar/(2m\omega)$, $\omega^2 = \Omega^2 + \frac{1}{4}\omega_c^2$, χ_{s_z} are spin functions, and

$$R_{nl}(x) = \sqrt{\frac{n!}{(n+|l|)!}} e^{-x/2} x^{\frac{|l|}{2}} L_n^{|l|}(x). \quad (4)$$

Note that, as expected, the dependence on θ indicates that electrons rotate clockwise when a magnetic field applied along the z -direction. However, it is convenient to define the z -component of single particle angular momentum as $\mathbf{l}_z = -\frac{1}{i}\frac{\partial}{\partial\theta}$ so that the eigenstates with positive

angular momenta have lower energy. The eigenenergies are

$$\epsilon_{nls_z} = \hbar\omega(2n + |l| + 1) - \frac{1}{2}\hbar\omega_c\ell - g\mu S_z B. \quad (5)$$

These eigenstate wavefunctions are labeled by quantum numbers of orbital states and the z -component of angular momentum (n, l) : Note that for a given $n = 0, 1, 2, \dots$ the quantum number l can take all possible integer values. It is useful to study properties of *zero* magnetic field single particle states. The eigenenergies are

$$\epsilon_{nl}^0 = \hbar\Omega(2n + |l| + 1). \quad (6)$$

These single particle energy levels ϵ_{nl}^0 can be degenerate, for example, (n, l) and $(n, -l)$. These degeneracies are such that they lead to the magic numbers of harmonic potential 2, 6, 12, etc. In the presence of a weak magnetic field along the z -axis *all* degeneracies will be lifted.

The many-body ground state Ψ of H is expanded in terms of Slater determinant states

$$\Psi = \sum_{\alpha} C_{\alpha} \Psi_{\alpha}, \quad (7)$$

where

$$\Psi_{\alpha} = c_{n_1 l_1 \sigma_1}^+ c_{n_2 l_2 \sigma_2}^+ \dots c_{n_N l_N \sigma_N}^+ \Psi_0. \quad (8)$$

Here $\alpha = \{n_1 l_1 \sigma_1, \dots, n_N l_N \sigma_N\}$ and labels a Slater determinant. Each creation operator $c_{nls_z}^+$ creates an electron in an eigenstate of *zero* magnetic field single particle Hamiltonian. The energy of Ψ_{α} is denoted by E_{α} , and it is the sum of energies of single particle states ϕ_{nls_z} . Even in the presence of a magnetic field we use the same many-body basis states as in zero magnetic field, with replacing Ω by ω . We found numerically that it is convenient to use these zero field particle states in constructing Slater determinants. The many-body Hilbert space can be divided into regions with different quantum numbers (S_z, L_z) : In each region we construct the many-body basis states which have the well-defined z -component of total angular momentum quantum number $L_z = \sum_{i=1}^N l_i$ and the z -component of total spin S_z . All possible eigenstates in the Hilbert space (S_z, L_z) are calculated, and the minimum energy state is found.

For numerical diagonalization of the Hamiltonian matrix, only Slater determinant basis states with energies $E_{\alpha} \leq q\hbar\omega$ are included, where $q = 20 - 25$. Typically, we have included about 3,000-14,000 basis states. We have checked that for these values q the energy differences between different states have converged. For example, when $N = 6$, $B = 0$ and $\hbar\Omega = 0.3\text{meV}$ the energy differences between the ground state $(0, 0)$ and one of the competing state $(2, 0)$ are 0.0371, 0.0332, 0.0328 meV for $q=21, 23, 25$, respectively. Results for $N = 3$ and 4 are in good agreement with the results of Mikhailov [7]. For example, for $\hbar\Omega = 0.118565$ (corresponding to $\lambda = 10$ in Ref. [7]), we have $E_{(1/2,1)}/\hbar\Omega = 17.6279$ ($N = 3$) and

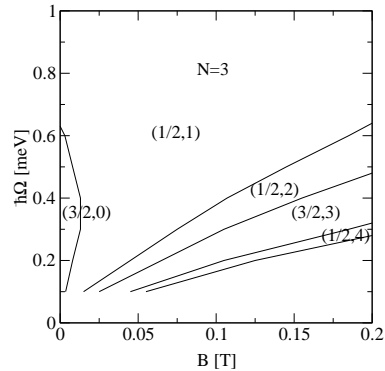


FIG. 1: Phase diagram for $N = 3$. Each state is denoted by the quantum numbers (S_z, L_z) . For strongly correlated regime (for small $\hbar\Omega$), the ground states are very sensitive to the magnetic field.

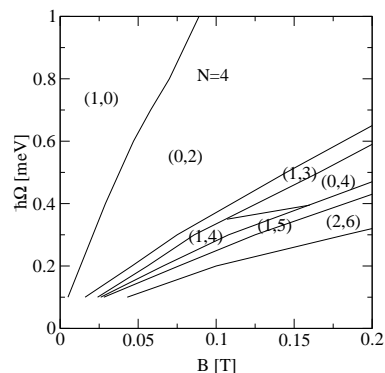


FIG. 2: Same as in Fig.1, but $N = 4$.

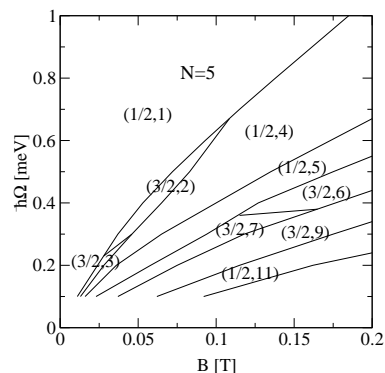


FIG. 3: Same as in Fig.1, but $N = 5$.

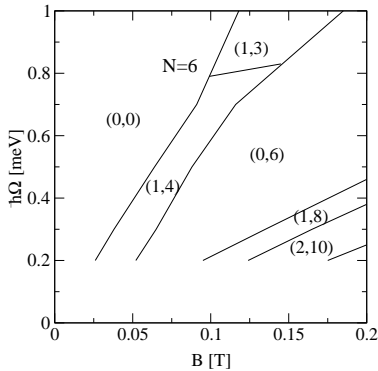


FIG. 4: Same as in Fig.1, but $N = 6$.

$E_{(1,0)}/\hbar\Omega = 31.4120(N = 4)$, perfectly consistent with the numbers in the reference. Note that when $\hbar\Omega$ gets too small more basis states need to be included and the numerical work becomes unwieldy. These results are not included in the phase diagrams.

Figures 1,2,3 and 4 show phase diagrams for $N = 3, 4, 5$, and 6 in the weak potential and magnetic field regime. Each phase is labeled by the total spin and angular momentum quantum numbers (S_z, L_z) . These phase diagrams are constructed schematically from the calculated energies of different (S_z, L_z) states at various values of $(\hbar\Omega, B)$. We took $B = 0, 0.01, \dots, 0.19, 0.2$ T for all values of N shown in the figures, and took $\hbar\Omega = 0.1, 0.2, \dots, 1.0$ meV for $N = 3, 4, 5$ while $\hbar\Omega = 0.2, 0.3, 0.5, 0.7, 1.0$ meV for $N = 6$. We remark on some of the qualitative aspects of these phase diagrams. (i) Note that some of the phase regions are divided into subregions separated by horizontal phase boundaries. Also we notice that some of the phase boundaries are linear functions of B . (ii) These figures show that, as the strength of the potential or magnetic field changes the ground state quantum number L_z changes *sensitively*. As the magnetic field B increases the value of L_z tend to increase. On the other hand as the strength of the confinement potential $\hbar\Omega$ increases the ground state L_z tend to decrease. (iii) Ground state energies obtained for $L_z = 0, 3, 4$, and 6 are, respectively, 37.28, 37.58, 37.88, and 38.05 meV (These values are for the parameters $N = 6, B = 0$, and $\hbar\Omega = 1.0$ meV). These results indicate that the ground states are nearly degenerate as a result of strong electron correlation.

We now discuss why some of the phase boundaries in Figures 1, 2, 3, and 4 are linear functions of B . It is useful to separate the total energy into

$$E_{tot} = E_{kin} + E_{diam} + E_{para} + E_{spin} + E_{int}, \quad (9)$$

where $E_{kin} = \langle \sum_i \epsilon_{n_{il}}^0 \rangle$ is the kinetic energy, $E_{diam} = \langle \sum_i \frac{1}{8} m^* \omega_c^2 r_i^2 \rangle$ is the diamagnetic energy,

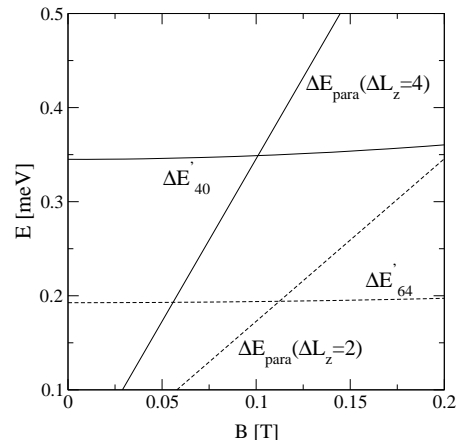


FIG. 5: Here we compare the differences $E_{para}(S_z, 2, L_z, 2) - E_{para}(S_z, 1, L_z, 1)$ and $E'(S_z, 1, L_z, 1) - E'(S_z, 2, L_z, 2)$ for states sharing the same phase boundary. Two solid lines represent the magnetic field dependence of $\Delta E_{para}(\Delta L_z = 4) = E_{para}(0, 0) - E_{para}(1, 4)$ and $\Delta E'_{40} = E'(1, 4) - E'(0, 0)$, and the other two dotted lines represent $\Delta E'_{para}(\Delta L_z = 2) = E_{para}(1, 4) - E_{para}(0, 6)$ and $\Delta E'_{64} = E'(0, 6) - E'(1, 4)$. When these pair of lines cross the ground state changes. Here $N = 6, \hbar\Omega = 0.7$ meV, and E_{spin} is ignored. Note that the differences in $E'(S_z, L_z)$ are almost constant as a function of magnetic field while the difference in $E_{para}(S_z, L_z)$ are significant.

$E_{para} = -\frac{1}{2}\omega_c L_z$ is the paramagnetic energy, E_{int} is the interaction energy, and $E_{spin} = -g\mu B S_z$ is the Zeeman energy. Note that $E_{kin} \propto \Omega$. We now compare E_{para} with the rest of the ground state energy, $E'(S_z, L_z) = E_{kin} + E_{diam} + E_{int}$, ignoring E_{spin} , which is very small compared to the others. For many states found in the phase diagrams the values of $E'(S_z, L_z)$ are nearly the same. This property reflects the delicate competition between different states, which is an indication that the quantum dot is in the strongly correlated regime. However, since E_{para} depends significantly on B , we expect ground states to change sensitively as a function of B . This is explained in detail in Figure 5. Phase boundaries in the parameter space $(\hbar\Omega, B)$ is roughly determined by the sum of kinetic and paramagnetic energies: Consider the phase boundary between ground states $(S_z, 1, L_z, 1)$ and $(S_z, 2, L_z, 2)$, then, since the values of $E'(S_z, i, L_z, i)$ are nearly the same, we expect $b\Omega_1 - \frac{1}{2}\omega_c L_{z,1} \approx b\Omega_2 - \frac{1}{2}\omega_c L_{z,2}$, which gives $\Omega_1 - \Omega_2 \approx \frac{\omega_c}{2b}(L_{z,1} - L_{z,2})$ (here b is the proportionality factor in the kinetic energy). This result indicates that some phase boundaries are approximately a linear function of B . Also the slope of such a phase boundary is proportional to the difference in the angular momentum $L_{z,1} - L_{z,2}$. These results are consistent with many phase boundaries in Figures 1, 2, 3, and 4, although there are

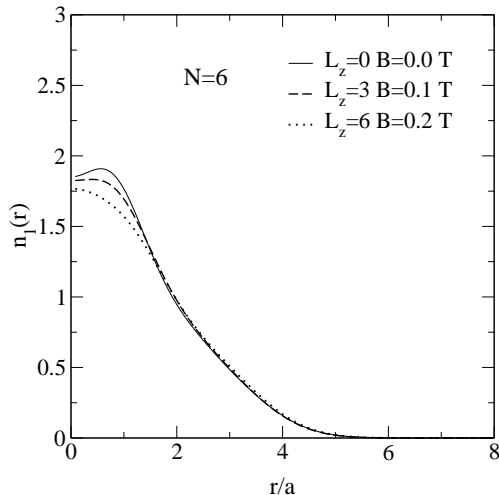


FIG. 6: Radial density profiles of several different ground-states with $S_z = 0$. Here $\hbar\Omega = 0.7\text{meV}$ and $N = 6$. For weak magnetic fields, radius of dot is roughly $5a$, where $a = \sqrt{\hbar/2m\omega}$. We notice that the profiles deviate slightly from each other. From these profiles we can estimate the density of 2D electron gas which these dots are made of to be about $9 \times 10^9\text{cm}^{-2}$.

few exceptions.

We now discuss some issues of experimental relevance. First we estimate the density of 2D electron gas which these dots can be made of. Figure 6 shows the radial electron density profile of dots for $N = 6$ when $\hbar\Omega = 0.7\text{meV}$. The radius of the dot is roughly $5a$ for weak fields considered in this paper. We have verified by integrating the density profile that the total number of electrons is N . For $m^* = 0.067m$, where m is the bare electron mass, the average electron density is approximately $9 \times 10^9\text{cm}^{-2}$. We suggest that our obtained phase diagrams may be explored experimentally by measuring the positions of cusps in the magnetic field dependence of chemical potential $\mu_N \equiv E_N - E_{N-1}$: Since ground state level crossings in the $N - 1$ and N electron systems lead respectively to positive and negative cusps, phase boundaries will show up as cusps in the chemical potential. We plot the magnetic field dependence of the chemical potentials μ_4 , μ_5 , and μ_6 , in Figure 7. We observe several cusps in Fig. 7, where $\hbar\Omega = 0.7\text{meV}$ is used. From our phase diagrams we can conclude that for smaller values of $\hbar\Omega$ many more cusps will show up in the magnetic field dependence of the chemical potential. Conductance peak spacings, given as the difference between the gate voltages, $V_g^{N+1} - V_g^N$, are related to the positions of the cusps: i.e. $e(V_g^{N+1} - V_g^N) \propto (\mu_{N+1} - \mu_N)$. The other

issue concerns that in real dots there may be some deviations from the perfect circular symmetry of the harmonic potential, and consequently degenerate single par-

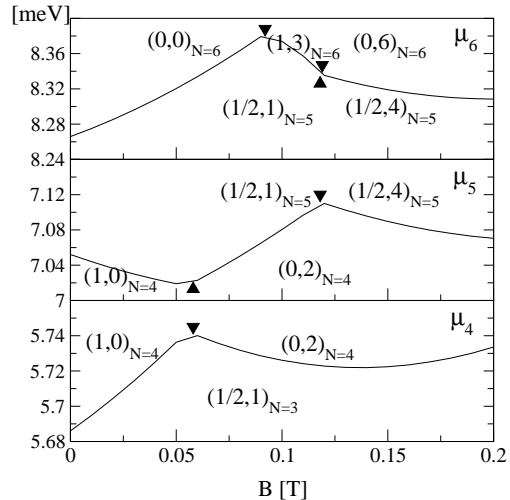


FIG. 7: Plot of the chemical potential $\mu_N \equiv E_N - E_{N-1}$ as a function of the magnetic field at $\hbar\Omega = 0.7\text{meV}$ for $N = 4, 5$, and 6 . The positions of magnetic fields, where a ground state level crossing in the $N - 1$ and N electron systems takes place, are indicated by \triangle and ∇ . The quantum states of the dots are denoted by (S_z, L_z) (The other cusp-like structures are artifacts of discrete data points).

ticle states of the harmonic potential at $B = 0$ may be absent. However, even in a harmonic potential electron-electron interactions will lift this degeneracy. Furthermore, the main conclusion of our work that the ground states change sensitively with B or $\hbar\Omega$ is not expected to be different since strong electron correlation is responsible for the sensitivity of ground states to the magnetic field and the strength of the confinement potential.

In this paper we explored quantum dots in a strongly correlated regime $R \gg 1$. Our exact diagonalization results show that the ground states of such quantum dots are rather sensitive to the magnetic field and strength of the confinement potential. We have predicted rich phase diagrams. Experimentally these phase diagrams may be explored by measuring the sensitive magnetic field dependence of the energy to add one electron to a dot, or by measuring the positions of conductance peak oscillations.

S.R.E.Y was supported by KOSEF through the Quantum-functional Semiconductor Research Center at Dongguk University and by grant R01-1999-00018-0 from interdisciplinary Research program of KOSEF.

-
- [1] For recent reviews, see: L.P. Kouwenhoven, D.G. Austing, and Tarucha, *Rep. Prog. Phys.* **64**, 701 (2001); L.P. Kouwenhoven and P.L. McEuen, in *Nano Science and Technology*, edited by G.Timp (Springer-Verlag, New York, 1999).
- [2] S.-R. Eric Yang, A. H. MacDonald, M.D. Johnson, *Phys. Rev. Lett.* **71**, 3194 (1993); A. H. MacDonald, S.-R. Eric Yang, and M.D. Johnson, *Aust. J. Phys.* **46** 345 (1993); S.-R. Eric Yang and A. H. MacDonald, *Phys. Rev. B*, **66**, 041304(R) (2002).
- [3] C. de C. Chamon and X.G. Wen, *Phys. Rev.* **49**, 8227 (1994); O. Klein, C. de C. Chamon, D. Tang, D.M. Abusch-Magder, U. Meirav, X.G. Wen, M.A. Kastner, S.J. Wind, *Phys. Rev. Lett.* **74**, 785 (1995); A. Karlhede, *et al.*, *Phys. Rev. Lett.* **77**, 2061 (1996); T. H. Oosterkamp, J. W. Janssen, L.P. Kouwenhoven, D. G. Austing, T. Honda, and S. Tarucha, *Phys. Rev. Lett.* **82**, 2931 (1999).
- [4] S. Tarucha, D. G. Austing, T. Honda, R.J. van der Hage, and L.P. Kouwenhoven, *Phys. Rev. Lett.* **77**, 3613 (1996); M. Koskinen, M. Manninen, and S. M. Reimann, *Phys. Rev. Lett.* **79**, 1389 (1997); S. Tarucha, D. G. Austing, Y. Tokura, W.G. van der Wiel, and L.P. Kouwenhoven, *Phys. Rev. Lett.* **84**, 2485 (2000).
- [5] L. Kouwenhoven and L. Glazman, *Phys. World* 14(1), 33, Jan. 2001 and references therein.
- [6] R. Egger, W. Hausler, C. H. Mak, and H. Grabert, *Phys. Rev. Lett.* **82** 3320 (1999); C. Yannouleas and U. Landman, *Phys. Rev. Lett.* **82** 5325 (1999); A. V. Filinov, M. Bonitz, and Y. E. Lozovik, *Phys. Rev. Lett.* **86** 3851 (2001); F. Selva and J.-L. Pichard, *Europhys. Lett.* **55**, 518 (2001).
- [7] S. A. Mikhailov, *Phys. Rev. B* **65**, 115 312 (2002); *Phys. Rev. B* **66**, 153 313 (2002).
- [8] E. Abrahams, S.V. Kravchenko, and M.P. Sarachik, *Rev. Mod. Phys.*, **73**, 251 2001.
- [9] D. Pfannkuche, V. Gudmundsson, and P.A. Maksym, *Phys. Rev. B* **47**, 2244 (1993).
- [10] P. A. Maksym and T. Chakraborty, *Phys. Rev. Lett.* **65**,108 (1990).
- [11] P. Hawrylak, *Phys. Rev. Lett.* **71**, 3347 (1993); J.J. Palacios, L. Martin-Moreno, G. Chiappe, E. Louis, and C. Tejedor, *Phys. Rev. B* **50**, 5760 (1994).
- [12] S. Siljamaki, A. Harju, R.M. Nieminen, V.A. Sverdlov, and P. Hyvonen; cond-mat/0112243.
- [13] S.M. Reimann, M. Koskinen, M. Manninen, and B.R. Mottelson, *Phys. Rev. Lett.* **83**, 3270 (1999); K. Hirose and N. S. Wingreen, *Phys. Rev. B*, **59**, 4604 (1999); M.-C. Cha and S.-R. Eric Yang, *Phys. Rev. B*, **61**, 1720 (2000).
- [14] V. Fock, *Z. Physik* **47**, 446 (1928).
- [15] C.G. Darwin, *Proc. Cambridge Philos. Soc.* **27**, 86 (1931).
- [16] P. A. Maksym and T. Chakraborty, *Phys. Rev. B* **45**, 1947 (1992).